Journal of Structural Biology 186 (2014) 302–307

Contents lists available at ScienceDirect

Journal of Structural Biology

journal homepage: www.elsevier.com/locate/yjsbi

Technical Note

2dx_automator: Implementation of a semiautomatic high-throughput high-resolution cryo-electron crystallography pipeline

Sebastian Scherer, Julia Kowal, Mohamed Chami, Venkata Dandey, Marcel Arheit, Philippe Ringler, Henning Stahlberg *

Center for Cellular Imaging and NanoAnalytics, Biozentrum, University of Basel, CH-4058 Basel, Switzerland

ARTICLE INFO

Article history:
Received 6 February 2014
Received in revised form 7 March 2014
Accepted 21 March 2014
Available online 28 March 2014

Keywords:
2dx
Image processing automation
Cryo-EM
Direct electron detector
High-throughput electron microscopy
Membrane proteins

ABSTRACT

The introduction of direct electron detectors (DED) to cryo-electron microscopy has tremendously increased the signal-to-noise ratio (SNR) and quality of the recorded images. We discuss the optimal use of DEDs for cryo-electron crystallography, introduce a new automatic image processing pipeline, and demonstrate the vast improvement in the resolution achieved by the use of both together, especially for highly tilted samples. The new processing pipeline (now included in the software package *2dx)* exploits the high SNR and frame readout frequency of DEDs to automatically correct for beam-induced sample movement, and reliably processes individual crystal images without human interaction as data are being acquired. A new graphical user interface (GUI) condenses all information required for quality assessment in one window, allowing the imaging conditions to be verified and adjusted during the data collection session. With this new pipeline an automatically generated unit cell projection map of each recorded 2D crystal is available less than 5 min after the image was recorded. The entire processing procedure yielded a three-dimensional reconstruction of the 2D-crystallized ion-channel membrane protein MloK1 with a much-improved resolution of 5 Å in-plane and 7 Å in the z-direction, within 2 days of data acquisition and simultaneous processing. The results obtained are superior to those delivered by conventional photographic film-based methodology of the same sample, and demonstrate the importance of drift-correction.

1. Introduction

The introduction of direct electron detectors (DEDs) featuring a radiation-hardened CMOS sensor (Bammes et al., 2012; Milazzo et al., 2011) to the field of cryo-electron microscopy (cryo-EM) has brought enormous advantages. The detective quantum efficiency (DQE) of these devices is significantly higher than that of charge-couple device (CCD) cameras or even photographic film (McMullan et al., 2009; Veesler et al., 2013). In general, images recorded on DEDs have a higher signal-to-noise ratio (SNR) and the highest contrast ever achieved. The highest DQE is thereby achieved by Gatan's K2 Summit camera due to its ability to count single electrons from its internal chip readout every 2.5 ms (Li et al., 2013a; Ruskin et al., 2013). The fast readout speed also makes it possible to record movie sequences rather than single images, allowing to split the electron dose over multiple exposures of the same region, resulting in a sequence of images. Although the SNR of the individual frames is much lower, the sample motion during exposure can still be followed and compensated for by frame-alignment and averaging (Brilot et al., 2012; Campbell et al., 2012), leading to impressive resolution improvements (Liao et al., 2013). Here, we discuss application of a DED to two dimensional (2D) membrane protein crystals.

Processing individual images of 2D crystals generally involves (i) defocus estimation, (ii) determination of the tilt-geometry, (iii) lattice estimation, (iv) lattice correction (unbending) to correct for crystal imperfections, (v) contrast transfer function (CTF) correction and (vi) averaging the data of one crystal into one unit-cell (Arheit et al., 2013c). When recording data on a CCD camera or on film, both the low SNR and the presence of beam-induced sample drift, make automatic processing of crystal data challenging and,

Abbreviations: 2D, two dimensions/dimensional; 3D, three dimensions/dimensional; CCD, charge coupled devices; CMOS, complementary metal-oxide-semiconductor; cryo-EM, cryo-electron microscopy; CTF, contrast transfer function; DED, direct electron detector; EM, electron microscope; DQE, detector quantum efficiency; GUI, graphical user interface; SNR, signal-to-noise ratio.

* Corresponding author. Address: Center for Cellular Imaging and NanoAnalytics (C-CINA), Biozentrum, University of Basel, WRO-1058, Mattenstrasse 26, CH-4058 Basel, Switzerland.

E-mail address: henning.stahlberg@unibas.ch (H. Stahlberg).

http://dx.doi.org/10.1016/j.jsb.2014.03.016
1047-8477/

in some cases, impossible. Manual processing and assessment of the quality of individual images is still the major bottleneck. Here, we present an automation pipeline that mostly eliminates this tedious work and ensures high-throughput, while exploiting the potential of DEDs, i.e., drift-correction of dose-fractioned exposure series. The processing pipeline is executed automatically at the EM, immediately after each movie/image has been acquired. The quality of the recorded images is displayed on a single user-friendly GUI via which the operator of the electron microscope (EM) can continuously optimize the microscope settings based on the results obtained. Both, the quality and the productivity of data acquisition sessions are tremendously increased by this fast, automated procedure. The performance of the new pipeline, in terms of time to solution and achieved resolution, is superior to that of any previous 2D crystal processing procedures.

2. Automation pipeline setup

The automation pipeline (Fig. 1) consists of five different stages: (i) movie/image acquisition, (ii) initial quality assessment on the microscope computer, (iii) automatic drift-correction (movie mode only), (iv) automatic image processing of individual crystals, and (v) manual 3D merging of the entire 2D crystal dataset. Storing a raw sequence of dose-fractioned movie frames (later called a stack) in a particular folder on the storage server triggers the processing procedure outlined above. The new pipeline automates the major bottleneck of the classical 2D crystal pipeline, namely the processing of a large number of 2D images (ideally more than 100). 3D merging is not a time intensive process, and requires operator decisions that can vary greatly between projects, such as detecting conformational variability among the 2D crystals, or choosing optimal lattice line fitting parameters. 3D merging therefore still is a manual process in our pipeline.

In our setup the operator of the EM records and stores the raw movie stack from the acquisition computer onto a network-attached storage server. Both, drift-correction and the automatic image processing run on a dedicated additional workstation. In this way, a 2D projection map is generated from a raw stack (25 frames, ~4k × ~4k pixels) in less than 5 min.

3. Data acquisition

The presented software was developed and optimized for the online processing of 2D crystal images recorded on a FEI Titan Krios equipped with a Gatan K2 Summit DED. In the experiments we report, the detector was operated in the electron counting-mode with an image size of ~4k × ~4k pixels. Following (Li et al., 2013a), we distributed the cumulated dose over 25 frames recorded over 5sec. We operated the microscope in low-dose mode at a nominal magnification of 22,500× at the screen level, resulting in an effective magnification of ~37,000× on the K2 chip (5 μm physical pixel size), which converts to a pixel size of 1.34Å on the sample level.

The pixel electron dose rate, used to image the sample was kept below 6 counts per pixel per second, in order to avoid coincidence loss due to undercounting (Li et al., 2013a). The cumulative dose applied to the sample for recording one image stack remained below ~16 electrons per Å^2.

The Gatan K2 summit detector can also be operated in the so-called 'super-resolution mode', where the physical ~4k × ~4k optical chip is modeled as an ~8k × ~8k device by sub-pixel precision hit-location interpolation. Li et al. record images in super-resolution mode and apply a "2 × 2-binning" by cropping in Fourier space to avoid aliasing (Penczek et al., 2014), before drift-correction and further image processing (Li et al., 2013b). Both, the better detector quantum efficiency of the K2 summit detector operated in super-resolution mode (Ruskin et al., 2013) and the fact that Fourier cropping of an ~8k × ~8k image into an ~4k × ~4k image prevents unfavorable aliasing of super-resolution data in Fourier space, favor the use of the super-resolution mode. Our drift-correction automation tool can deal with both stacks of ~4k × ~4k frames as well as stacks of ~8k × ~8k frames, as long as the latter are automatically binned before processing (Liao et al., 2013). It corrects the drift of entire frames during the exposure. Use of super-resolution imaging on a Gatan K2 summit DED would further improve the DQE at high resolution, which would also benefit single particle refinement to correct for local varying tilt geometries of the 2D crystals (Scherer et al., 2013).

4. Drift-alignment of individual frames

Sample drift during exposure to the electron beam can be corrected in the movie mode by aligning all frames and then averaging to obtain a drift-corrected average. There are different algorithmic approaches to the frame-alignment problem. The alignment method developed by Li et al. (Li et al., 2013b) features some algorithmic advantages compared to the straight-forward alignment of adjacent frames integrated into Gatan's acquisition software. Instead of aligning adjacent frames with respect to each other, Li et al. determine the local offsets between adjacent and also non-adjacent frames, which leads to an over determined system of linear equations. The optimal shifts with respect to a 'global cross-correlation' can be determined from the least square solution of this system of equations. In our hands the method developed by Li et al. showed more stable behavior than Gatan's acquisition software. In order to overcome the beam-induced motion of the sample at the beginning of an exposure and 'shutter opening' artifacts, like Li et al. we recommend removing the first two frames from the

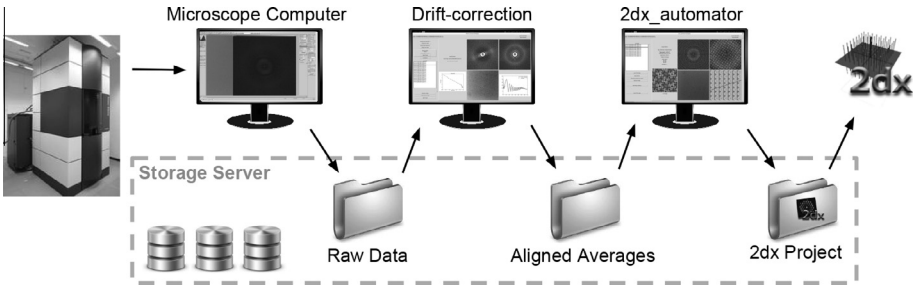

Fig.1. Automation pipeline. Images are recorded with the EM using a DED operated in movie mode. Saving image stacks to the storage server triggers the drift-correction implemented by (Li et al., 2013b). The corrected average is automatically moved to another folder on the storage server, which triggers the automatic image processing by *2dx_automator*. *2dx* adds the drift-corrected image into the existing project and processes the image based on the project-wide parameters. Once all individual images have been processed and if required manually optimized, *2dx_merge* is used to merge the entire dataset in 3D.

raw stacks and only aligning and averaging the 23 remaining frames (Li et al., 2013b).

To enable real-time drift-correction, we developed new automation software equipped with a graphical user interface (GUI; Fig. 2A), which employs the drift-correction toolkit by (Li et al., 2013b). Our new tool periodically checks for arrival of a new raw image stack in an input directory, and then launches drift-correction on the stack to produce a frame-aligned average image in an output directory. The GUI of this tool (Fig. 2A) shows (i) the power spectrum of the raw average, (ii) the power spectrum of the drift-corrected average, (iii) the drift-corrected average extracted from the corrected stack, (iv) the rotationally averaged power spectra of the raw and corrected averages as one-dimensional plots, and (v) the applied shifts as a 2D plot. This new automation GUI can also be used to automatically drift-correct movie-mode images recorded for single particle and helical reconstruction projects.

5. Automatic image processing in *2dx*

Drift-corrected images are then automatically processed by *2dx*. The starting point for the presented automatic crystal image processing is hereby a configuration file providing generic parameters applicable to all images of the project. These parameters are obtained by manually processing a few images with *2dx_image* and defining the optimized parameters as default values for subsequent automatic runs. The software offers a set of exemplary configuration files and allows loading of own configuration files from other projects, which facilitates the initial tuning significantly. The use of DEDs significantly simplifies finding commonly applicable processing parameters. Automation was successful for all so far tested membrane protein projects ($n > 3$), while it often failed before the introduction of DEDs due to the lower quality of the images.

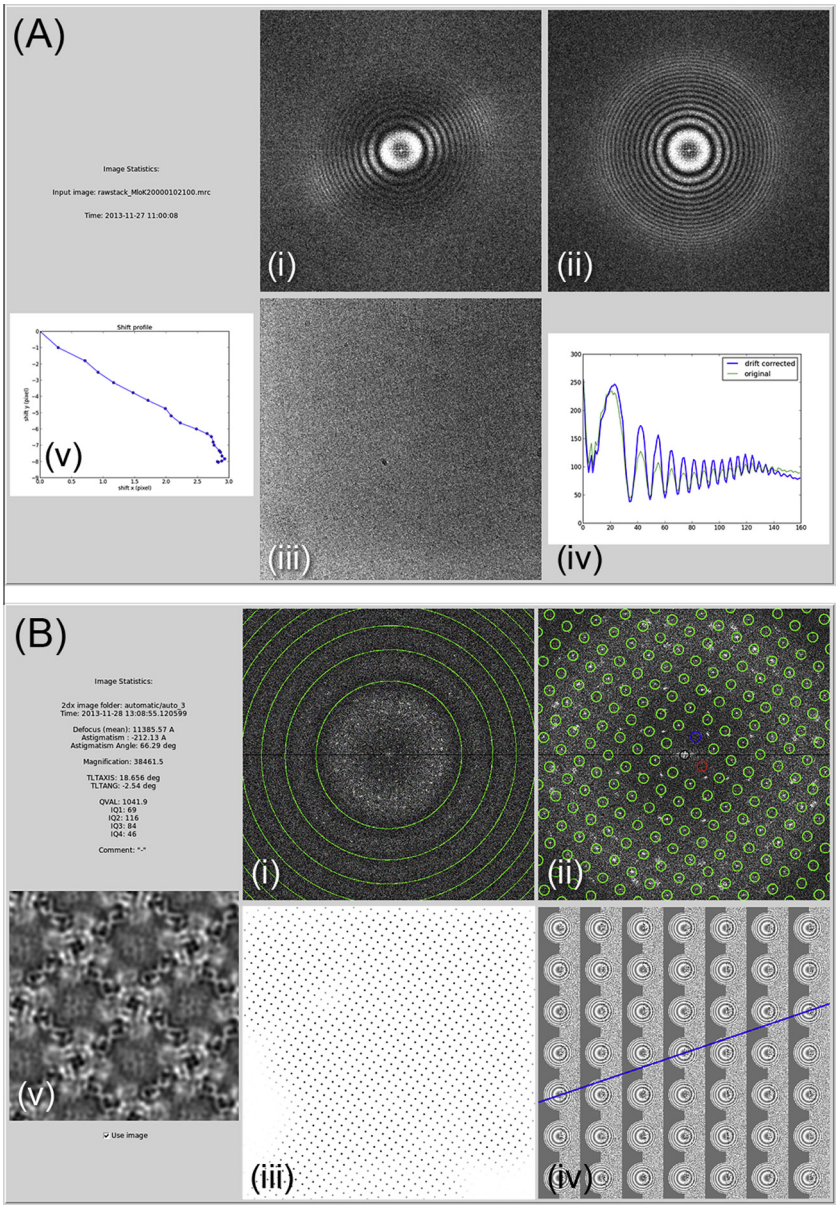

Fig.2. Automation GUIs. (A) Drift-correction GUI (assessment part). (i) power spectrum of the raw average, (ii) power spectrum of the drift-corrected average, (iii) drift-corrected average image, calculated from the corrected image stack, (iv) rotationally-averaged power spectrum of the raw and corrected image averages as one-dimensional plots, and (v) the applied shifts as a 2D plot. Based on the power spectra of the raw and drift-corrected averages, the user can judge the quality of the recorded image and the effect of the drift-correction. Additionally we provide a plot of the applied in-plane shift and a binned version of the corrected average. (B) Diagnostic view of the *2dx_automator* GUI. (i) Fourier transform with Thon rings and (ii) fitted lattice, (iii) peak profile from the unbending step used to mask the image, (iv) locally estimated defocus values, (v) final 2D projection map.

The first step of image processing in *2dx* is to estimate the defocus values of each micrograph. This is done using a slightly adapted version of CTFFIND3 (Mindell and Grigorieff, 2003) that is fully integrated in *2dx*. We suggest searching for astigmatic defocus values within 0.5–5.0 μm in steps of 250 Å. Based on this range, CTFFIND3 was able to find the correct defocus parameters for all tested images.

As the automation does not know 'a priori' whether a particular image shows a tilted or non-tilted crystal, our automation treats all images as if they show a tilted sample and determines the tilt-geometry of each as detailed in (Arheit et al., 2013b). Due to the new detector and the significant improvements of the version from 2013 of CTFFIND3, the success rate of this procedure is almost 100% (Section 6).

The remaining processing tasks: (i) lattice determination (Zeng et al., 2007), (ii) crystal unbending, (iii) CTF-correction and (iv) map-generation, are automatically conducted in exactly the same way as for a classical *2dx*-project (Arheit et al., 2013c).

The automation pipeline also offers the possibility to test for potential second crystallographic lattices in the crystal images, which can then be processed within 2dx either fully automatically or manually. As most crystals do not cover the entire image, masking during the processing improves the final 2D projection map. Automatic masking is now included in the pipeline and achieved by applying binary morphologic operations to the peak-profile generated by the *2dx*-script *UnbendII*.

Even some images recorded on a DED cannot be processed automatically and require manual intervention or fine-tuning at some points. In order to check the result of the automatic processing pipeline, we have implemented a GUI (termed *2dx_automator*) that displays several useful diagnostic graphs and figures (Fig. 2B); these include (i) an overview of processing parameters such as the determined tilt geometry and IQ statistics, (ii) Fourier transform with fitted Thon rings, and (iii) fitted lattice, (iv) peak-profile from the unbending step used to mask the image, (v) locally estimated defocus values indicated by Thon ring fits from local CTFFIND3 runs on 7×7 sub-tiles of the image, and (vi) the final 2D projection map. From this information, the operator can judge the reliability and quality of the automatic processing. Further, when processing fails the provided information can be used to detect, which particular processing step needs manual intervention.

To provide a complete overview of the data recorded and automatically processed, we have implemented a 'project statistics overview' chart (Supplementary Fig. 1). This informs the user about the recorded sample tilts, the recorded defocus values dependent on sample tilt, and about the determined quality values (QVal) (Gipson et al., 2007a,b). From this overview the user operating the EM can see which data are still missing with respect to tilt angles and defocus settings. Thus, our software greatly facilitates the collection of data at all of the required settings, leading to high quality 3D reconstructions in terms of resolution and completeness.

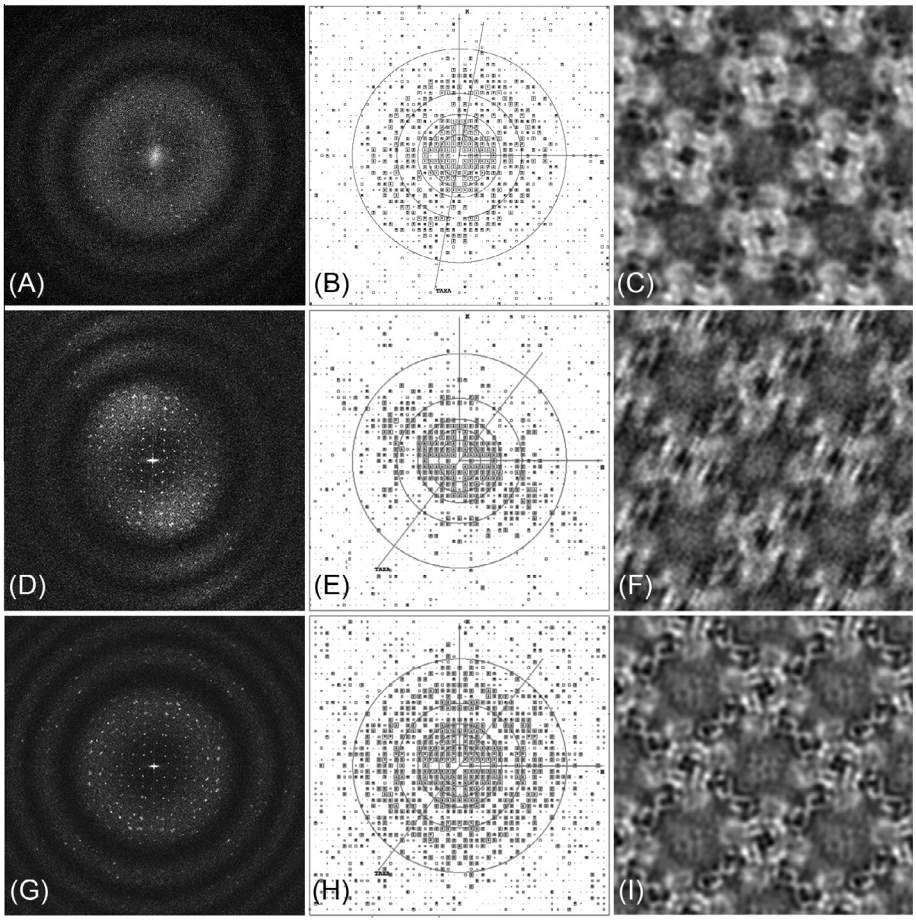

Fig.3. Impact of DEDs and drift-correction on 2D electron crystallography projection maps generated from a non-tilted crystal. (A–C) are for a crystal imaged on photographic film. (A) Power spectrum of an image. (B) Resolution circle plot from the canonical lattice showing the quality of the diffraction spots. Circles correspond to 36 Å, 24 Å, 18 Å, 12 Å and 7 Å, the border is at 5 Å. (C) Reconstructed unit-cell (2×2 unit cells are shown). (D–F) same as for (A–C) but a DED recording without drift-correction. The resolution loss due to drift is visible. (G–H) raw data used for (D–F) but with drift-correction before crystallographic image processing. The results for the crystals recorded on the DED (D–F) were obtained without manually tuning the processing.

6. Application to a MloK1 membrane protein dataset

In order to test the new automation pipeline, we imaged 2D crystals of the potassium channel membrane protein MloK1 (131 × 131 Å unit cell size, $P42_12$ symmetry, 1–3 μm diameter of 2D crystals, vitrified on thin carbon films supported by holey carbon film; (Kowal et al., 2014)) using a Titan Krios microscope equipped with a Gatan K2 summit DED as described above. The automation pipeline was setup so that storing a raw stack to a particular folder triggered automatic drift-correction followed by automatic image processing by *2dx_automator*. We recorded and automatically processed 148 MloK1 images with 0°–45° nominal sample tilt within two days. We observed a 100% success rate for drift-correction, defocus determination and tilt-geometry determination based on the measured defocus gradient. In ~4% of all cases (6 images out of 148), manual lattice determination was required, because the automatic lattice determination based on the program *FindLattice* (Zeng et al., 2007) failed. The average time required to obtain a 2D projection map was below 5 min.

The processing results obtained using images of MloK1 crystals recorded on photographic film and by DED (without and with drift-correction) are shown and compared in Fig. 3 and Supplementary Fig. 4. Crystal images recorded on film show diffraction spots with acceptable SNRs and with a fairly high completeness up to 9 Å, whereas the drift-corrected image recorded on Gatan's K2 summit DED show similar completeness out to 5 Å. Projection maps generated from images recorded on the DED show more features and allow easier identification of individual helices. These data also show that drift-correction on tilted 2D crystals is central to the success of electron crystallography.

7. Towards overcoming the beam-induced resolution loss for highly tilted samples

Recording and aligning movie images does not overcome beam-induced resolution loss completely, as local movements within the crystals are not addressed by this approach (Glaeser et al., 2011). Beam-induced movement has a stronger impact on images of tilted samples than of non-tilted samples, due to a beam-induced physical up- or downwards movement of the sample and due to charge-induced deflection of the beam. Drift-correction therefore has a much greater impact still on image sequences recorded on tilted 2D crystals (Supplementary Fig. 2), where we often obtained isotropic resolution up to at least 7 Å in all directions also on tilted samples. Correcting the drift between dose-fractioned frames of one exposure is an easy and effective way to almost eliminate beam-induced resolution loss. Crystal unbending applied to the individual frames, i.e., 'movie-mode unbending', would further overcome the beam-induced local movements within the imaged 2D crystals (Glaeser et al., 2011).

8. 3D reconstruction

We manually merged the best 65 of the 148 recorded and automatically processed images to obtain a 3D reconstruction, following the approach described in (Arheit et al., 2013a). Different quality assessments are shown in Supplementary Table 1 and Fig. 3. The resolution of the DED reconstruction (5/7 Å) is significantly higher than the resolution obtained when photographic film was used (7/12Å) (Kowal et al., 2014), as also evident in Fig. 4. The most important difference, however, is the time required to produce these two reconstructions: Several months (>10) of work in data collection and processing over a period of 3 years were required for the data recorded on photographic film, whereas the DED study took only two days of data collection and processing, demonstrating the superiority of the new procedure.

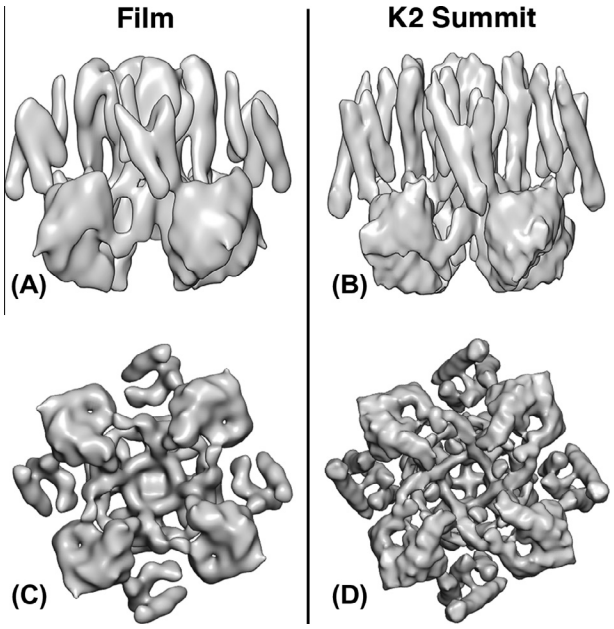

Fig.4. Comparison of the MloK1 3D reconstructions obtained from photographic film (A, C; >10 months of work) and DED (B, D; 2 days of work). A, B: Membrane view. C, D: Cytoplasmic view of the reconstruction. The resolution obtained using the DED was higher.

9. Conclusions and future developments

The presence of high-order diffraction spots in the power spectra of the drift-corrected average, even for highly tilted samples, the almost 100% success rate of the automatic processing pipeline, and the quality of the 3D reconstruction, prove that the new automation pipeline and the new software outperform all previously available procedures in terms of usability, time to solution, and achieved resolution.

The drift-correction method used in the new automation pipeline accounts for displacements of entire frames, but not for local movements within sub-areas of the image. Correcting these local displacements, so-called movie-mode unbending, would further increase the achieved resolution. When targeting a resolution significantly below 5 Å for non-tilted samples, careful microscope alignment, parallel sample illumination and computational correction for on-axial beam-tilt effects are indispensable. Images of crystals recorded at high sample tilt have to be corrected for titled-transfer function effects (Henderson et al., 1986), the use of which is implemented in 2dx. Limitations due to not perfectly flat crystals, especially when working with 2D crystals vitrified in buffer solution, can be overcome by applying a 3D single particle processing approach to individual proteins of a 2D crystal (Scherer et al., 2013). Any limited order in the imaged 2D crystals, however, will likely remain the resolution-limiting factor in the structure determination.

Acknowledgments

We thank Shirley A. Müller for insightful discussions and critically reading of the paper, and Pawel A. Penczek, Werner Kühlbrandt, Cristina Paulino, and Deryck Mills for fruitful discussions. This work was supported by the Swiss National Science Foundation

(grants 315230_146929, 205320_144427, and the NCCR TransCure). We acknowledge generous support by the FAG Basel.

All the here-described procedures are implemented in the *2dx* package, which is available on www.2dx.org.

Appendix A. Supplementary data

Supplementary data associated with this article can be found, in the online version, at http://dx.doi.org/10.1016/j.jsb.2014.03.016.

References

Arheit, M., Castano-Diez, D., Thierry, R., Abeyrathne, P., Gipson, B.R., et al., 2013a. Merging of image data in electron crystallography. Methods Mol. Biol. 955, 195–209.

Arheit, M., Castano-Diez, D., Thierry, R., Gipson, B.R., Zeng, X., et al., 2013b. Automation of image processing in electron crystallography. Methods Mol. Biol. 955, 313–330.

Arheit, M., Castano-Diez, D., Thierry, R., Gipson, B.R., Zeng, X., et al., 2013c. Image processing of 2D crystal images. Methods Mol. Biol. 955, 171–194.

Bammes, B.E., Rochat, R.H., Jakana, J., Chen, D.H., Chiu, W., 2012. Direct electron detection yields cryo-EM reconstructions at resolutions beyond 3/4 Nyquist frequency. J. Struct. Biol. 177, 589–601.

Brilot, A.F., Chen, J.Z., Cheng, A., Pan, J., Harrison, S.C., et al., 2012. Beam-induced motion of vitrified specimen on holey carbon film. J. Struct. Biol. 177, 630–637.

Campbell, M.G., Cheng, A., Brilot, A.F., Moeller, A., Lyumkis, D., et al., 2012. Movies of ice-embedded particles enhance resolution in electron cryo-microscopy. Structure 20, 1823–1828.

Gipson, B., Zeng, X., Stahlberg, H., 2007a. 2dx_merge: data management and merging for 2D crystal images. J. Struct. Biol. 160, 375–384.

Gipson, B., Zeng, X., Zhang, Z., Stahlberg, H., 2007b. 2dx—User-friendly image processing for 2D crystals. J. Struct. Biol. 157, 64–72.

Glaeser, R.M., McMullan, G., Faruqi, A.R., Henderson, R., 2011. Images of paraffin monolayer crystals with perfect contrast: minimization of beam-induced specimen motion. Ultramicroscopy 111, 90–100.

Henderson, R., Baldwin, J.M., Downing, K.H., Lepault, J., Zemlin, F., 1986. Structure of purple membrane from halobacterium halobium: recording, measurement and evaluation of electron micrographs at 3.5 Å resolution. Ultramicroscopy 19, 147–178.

Kowal, J., Chami, M., Baumgartner, P., Arheit, M., Chiu, P.L., et al., 2014. Ligand-induced structural changes in the cyclic nucleotide-modulated potassium channel MloK1. Nat. Commun. 5, 3106.

Li, X., Zheng, S.Q., Egami, K., Agard, D.A., Cheng, Y., 2013a. Influence of electron dose rate on electron counting images recorded with the K2 camera. J. Struct. Biol. 184, 251–260.

Li, X., Mooney, P., Zheng, S., Booth, C.R., Braunfeld, M.B., et al., 2013b. Electron counting and beam-induced motion correction enable near-atomic-resolution single-particle cryo-EM. Nat. Methods 10, 584–590.

Liao, M., Cao, E., Julius, D., Cheng, Y., 2013. Structure of the TRPV1 ion channel determined by electron cryo-microscopy. Nature 504, 107–112.

McMullan, G., Chen, S., Henderson, R., Faruqi, A.R., 2009. Detective quantum efficiency of electron area detectors in electron microscopy. Ultramicroscopy 109, 1126–1143.

Milazzo, A.C., Cheng, A., Moeller, A., Lyumkis, D., Jacovetty, E., et al., 2011. Initial evaluation of a direct detection device detector for single particle cryo-electron microscopy. J. Struct. Biol. 176, 404–408.

Mindell, J.A., Grigorieff, N., 2003. Accurate determination of local defocus and specimen tilt in electron microscopy. J. Struct. Biol. 142, 334–347.

Penczek, P.A., Fang, J., Li, X., Cheng, Y., Loerke, J., et al., 2014. CTER-rapid estimation of CTF parameters with error assessment. Ultramicroscopy 140C, 9–19.

Ruskin, R.S., Yu, Z., Grigorieff, N., 2013. Quantitative characterization of electron detectors for transmission electron microscopy. J. Struct. Biol. 184, 385–393.

Scherer, S., Arheit, M., Kowal, J., Zeng, X., Stahlberg, H., 2013. Single particle 3D reconstruction for 2D crystal images of membrane proteins. J. Struct. Biol..

Veesler, D., Campbell, M.G., Cheng, A., Fu, C.Y., Murez, Z., et al., 2013. Maximizing the potential of electron cryomicroscopy data collected using direct detectors. J. Struct. Biol. 184, 193–202.

Zeng, X., Gipson, B., Zheng, Z.Y., Renault, L., Stahlberg, H., 2007. Automatic lattice determination for two-dimensional crystal images. J. Struct. Biol. 160, 353–361.